

Nuclear-magnetic-resonance study of dislocation effects and axial compression effects in cesium iodide single crystals*

G. R. Gerhart[†]

Department of Physics, Wayne State University, Detroit, Michigan 48202

H. O. Hooper

Department of Physics, University of Maine at Orono, Orono, Maine 04473

(Received 16 July 1973; revised manuscript received 24 June 1974)

The intensity of the ^{127}I NMR in single crystals of CsI obtained from Harshaw Chemical Co. has been examined as a function of the orientation of the crystals with respect to the external magnetic field. The intensity varies due to the changing amount of first-order quadrupole broadening of the ^{127}I NMR line as a crystal is rotated in the magnetic field. A theoretical analysis of this intensity variation in terms of oriented dislocations has been carried out and indicates that preferentially oriented edge and screw dislocations with a [100] slip direction is consistent with the observed intensity variation for CsI. Uniaxial stress has been applied to single crystals of CsI producing broadening of the ^{127}I NMR line. From the observed broadening one component of the gradient elastic tensor, $C_{44} = 16 \times 10^3$ statvolt/dyn, has been determined.

I. INTRODUCTION

Several experiments have been carried out during the last twenty years to examine the nuclear electric quadrupole effects in single alkali halide crystals. Watkins and Pound¹ observed the intensities of the ^{79}Br , ^{81}Br , and ^{127}I lines to be very nearly equal to the $m = \frac{1}{2} \leftrightarrow m = -\frac{1}{2}$ transitions alone. The diminution of intensity was attributed to a distribution of splittings of the satellite transitions by electric quadrupole interactions. Hon and Bray² reported the existence of an anomalous peak in the angular dependence for the intensity of the ^{127}I NMR line in NaI and KI. Subsequent experiments and calculations by Hooper and Bray³ confirmed that oriented dislocations cause the anomalous electric field gradients in NaI. More recently Astrue and Hooper⁴ determined the gradient elastic constants, C_{11} and C_{44} , for NaI and concluded that the large ratio of C_{44}/C_{11} in the presence of oriented dislocations was responsible for the presence of the large anomalous resonance intensity when the external magnetic field was along a [100] crystallographic direction.

The first-order correction to the quadrupole interaction of the nuclear dipole-dipole interaction has been calculated by Volkoff, Petch, and Smellie⁵

$$(\Delta\nu)_m = \nu_{m \rightarrow m-1} - \nu_0 = \frac{3}{4} \left(\frac{2m-1}{I(2I-1)} \right) \frac{eQ}{h} \phi_{z'z'} \quad (1)$$

The individual transition frequency is $\nu_{m \rightarrow m-1}$, $\phi_{z'z'}$ is the component of the electric-field-gradient (EFG) tensor where z' is parallel to the applied magnetic field H_0 , and eQ is the nuclear electric

quadrupole moment. The EFG component $\phi_{z'z'}$ can further be expressed in terms of the EFG tensor components

$$\phi_{z'z'} = A_x + B_x \cos 2\theta_x + C_x \sin 2\theta_x, \quad (2)$$

where

$$A_x = \frac{1}{2} K(\phi_{yy} + \phi_{zz}) = -\frac{1}{2} K\phi_{xx}, \quad C_x = -K\phi_{yz},$$

$$B_x = \frac{1}{2} K(\phi_{yy} - \phi_{zz}), \quad K = \frac{3(2m-1)}{2I(2I-1)} \frac{eQ}{h}.$$

In Eq. (2) the x axis is parallel to the axis of rotation of the crystal in the magnetic field. The angle of rotation θ_x is zero when y is parallel to H_0 . Similar expressions for y and z rotations are obtained by cyclically permuting the xyz indices in Eq. (2). The EFG tensor ϕ_{xyz} can be determined completely by observing the angular variations in $\phi_{z'z'}$ for the three mutually perpendicular rotation axes.

The present work was undertaken to study the angular dependence of the ^{127}I NMR in single crystals of CsI. Since the preferred orientation of dislocations in body-centered cubic CsI is different from that in the face-centered cubic NaI and KI, a comparison of the anomalous angular dependences of the intensity of the NMR lines from these crystals was made to provide further evidence of the effect of oriented dislocations.

II. EXPERIMENTAL APPARATUS

The apparatus consisted of a Pound-Watkins⁶ NMR spectrometer, a detailed description of which can be found in Ref. 4. Several CsI single crystals obtained from the Harshaw Chemical Co. were

cylindrical in shape, $\frac{5}{16}$ in. in diameter, and $\frac{1}{2}$ in. long; the axes of cylindrical symmetry were parallel to [100] and [110] directions. Several additional unoriented pieces of single CsI crystals were studied and were also grown by the Harshaw Chemical Co. The unoriented pieces were x rayed and cut into rectangularly shaped samples with the sample sides being (100) or (110) planes.

III. ANGULAR DEPENDENCE EXPERIMENTS

The angular dependence of the ^{127}I resonance in NaI and KI single crystals has previously been reported for rotations about [100] and [110] axes.^{2,3} Similar experiments are reported here for the ^{127}I resonance in CsI single crystals.

The experimental data consist of first-derivative curves of NMR absorption spectra and it is estimated that the peak-to-peak (p-p) height of the derivative curves are determined to an uncertainty of about $\pm 1\%$ while the uncertainty in the peak-to-peak linewidth was approximately $\pm 5\%$. Repeated trials of NMR spectra under practically identical conditions showed a variation of about $\pm 10\%$ in measurements of the integrated intensity.

In Fig. 1 the total integrated intensity is shown for a [100]-type crystal; that is, a cylindrical crystal whose axis of rotation is a [100]-type crystallographic direction resulting in external magnetic field lying in a (100) plane. The angular dependence shown in Fig. 1 has maxima which occur 90° apart at angles corresponding to H_0 parallel to [100]-type crystallographic directions. The same type of angular dependence was previously observed^{2,3} for the ^{127}I resonance in [100] NaI and KI crystals. The ratio between the maximum and minimum values for the total integrated intensity ranged from 1.0 to 1.8 for CsI. The variations in these ratios from sample to sample are attributed to differences in alignment of the axis of each crystal and to variations in the defect structure in the crystals. The best oriented crystal had maxima separated by $90^\circ \pm \frac{1}{2}^\circ$ while the more poorly oriented crystals were misaligned by 3° to 5° .

The variations in the angular dependence of NMR spectra from the alkali halides originate from two main sources,^{7,8} quadrupole and nuclear dipole-dipole interactions. The quadrupole interaction causes a variation in the total integrated intensity of the NMR spectra while the dipole-dipole interactions are smaller and cause observable changes only in the angular dependence of the p-p height of the resonance line, not altering the intensity of the resonance.

The ratio of the maximum intensity observed at any angle of rotation in a [100] crystal to the

minimum intensity observed for CsI crystals was much smaller than the corresponding ratio for NaI. For NaI this ratio³ of the total integrated intensity when H_0 is parallel to [100] to the minimum intensity occurring at the trough of the angular dependence of the integrated intensity curve is very close to 3.9, showing some variation from crystal to crystal. The largest possible value for this ratio would be 3.9 if all of the satellite transitions have been split out from ν_0 to such an extent that only the $m = \frac{1}{2} \rightarrow m = -\frac{1}{2}$ central component is observed at that angle where I is a minimum and if all the satellite lines contribute to the intensity at the angle where I is a maximum. This ratio for the best aligned CsI [100] crystal was approximately 1.8.

The integrated intensity for the [100] CsI samples differs dramatically from the [110] samples (Fig. 2). The magnetic field H_0 moves in a (110) plane as the crystal is rotated about an [110] axis; therefore, H_0 is parallel to [100]-, [110]-, and [111]-type directions as the crystal is rotated through 180° . Figure 2 shows large maxima when H_0 is parallel to a [111] direction. A smaller maxima also occurred when H_0 is parallel to a [100] direction, although, this peak was observable only in the best oriented [110] samples. The corresponding data^{2,3} for [110] rotations in NaI and KI did not indicate the presence of a [111] intensity anomaly.

Large wings appear on the derivative curves when H_0 is within 15° of being parallel to a [111] direction. These wings are quite prominent even when H_0 is parallel to a [111] direction, indicating that the quadrupole splitting does not vanish completely at this orientation. If the splitting did vanish, the ratio of the maximum to minimum inte-

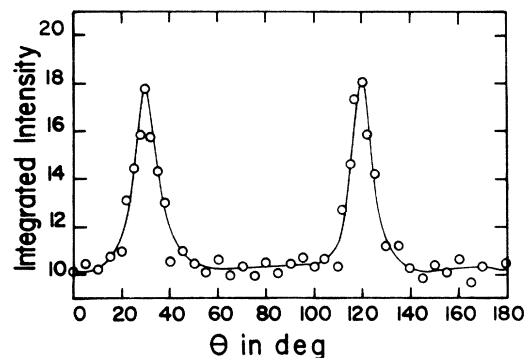


FIG. 1. Integrated intensity vs angle of rotation for ^{127}I in a CsI single crystal as the crystal is rotated about a [100] direction normal to H_0 . The angles $\theta = 30^\circ$ and $\theta = 120^\circ$ are [100]-type crystallographic directions.

grated intensity should be near the theoretical limit of 3.9, instead of the experimentally observed value of 2.4.

IV. AXIAL-COMPRESSION EXPERIMENTS

Several CsI cylindrical samples were axially compressed in the magnetic field and the changes in their NMR lines were observed under the applied stresses.

The compression experiments were performed with H_0 parallel to $[111]$ and $[100]$ directions. The applied stress introduces electric field gradients which cause the satellite transitions to split, broadening the resonance line and reducing the peak-to-peak (p-p) height. The p-p height of the derivative curve decreased while the linewidth ($\Delta\nu$) increased as the applied stresses were increased. At first the process was reversible, indicating that the elastic limit of the crystal had not been exceeded. The stress was increased until a permanent deformation of the solid was achieved. In a few cases, the crystals were compressed further in a plastic manner until a lower limit on the total integrated intensity of the line was reached.

Three separate $[100]$ samples of CsI were uniaxially compressed with H_0 parallel to a $[100]$ direction. The applied stress was increased gradually up to a value of 2×10^7 dyn/cm². A very slight decrease in the p-p height was first observed at an applied stress of 1.3×10^7 dyn/cm². It is believed that this value exceeded the elastic limit or yield point for CsI. The magnitude of these changes in the p-p height were very close to the limits im-

posed by experimental error, and it was difficult to achieve reproducibility of the experimental results.

The small changes in the NMR line for a $[100]$ compression in CsI, as compared to the rather large changes³ for NaI, can be readily explained. When H_0 is parallel to $[100]$ in NaI, essentially all of the satellites are in the central part of the ¹²⁷I NMR line. A fairly small stress will produce a substantial broadening of the NMR line resulting in a relatively large change in the p-p height. The corresponding p-p changes in the CsI are much smaller because fewer of the satellite transitions are in the central part of the NMR line.

Results of compression of a $[110]$ CsI crystal with H_0 parallel to a $[111]$ axis are shown in Fig. 3. The compression curve can be divided roughly into two regions. The first region ranges from zero to an applied stress of 9×10^6 dyn/cm². This region is elastic and the p-p height varies linearly with the applied stress. The second region extends beyond an applied stress of 9×10^6 dyn/cm², and it is the region of plastic deformation. The curve is no longer linear and the plastic deformations are not reversible, as indicated by the dashed line. The numbers above the data points in Fig. 3 indicate the sequence in which they were recorded during the compression experiments.

V. GRADIENT-ELASTIC CONSTANTS

The formalism of the gradient-elastic tensor was first developed by Shulman, Wyluda, and Anderson.⁹ The EFG tensor components, ϕ_{ij} , in a relatively strain-free cubic crystal are quite small for zero applied stress. To a first approximation

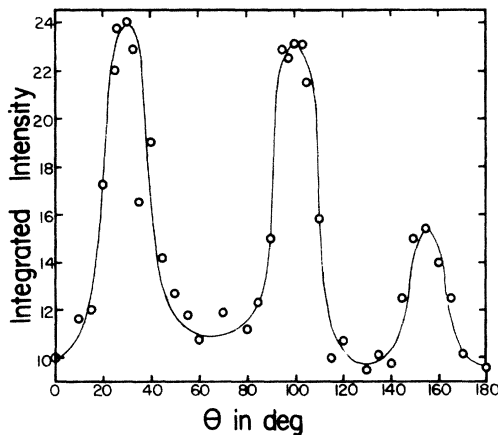


FIG. 2. Integrated intensity vs angle of rotation for ¹²⁷I in a CsI single crystal as the crystal is rotated about a $[110]$ direction normal to H_0 . The angles $\theta = 30^\circ$ and $\theta = 100^\circ$ are $[111]$ -type crystallographic directions.

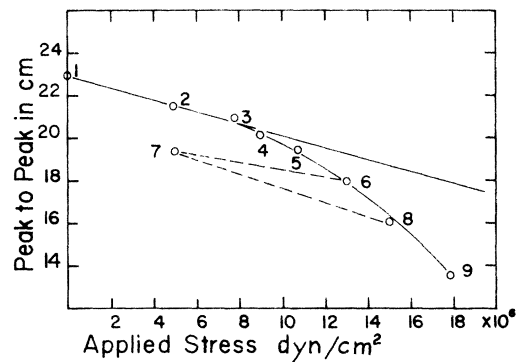


FIG. 3. Peak-to-peak height of the derivative curve for ¹²⁷I resonance vs applied stress for compression along a $[110]$ direction with H_0 in the plane normal to this direction of compression and aligned with a $[111]$ -type direction.

the ϕ_{ij} are linearly related to applied-stress tensor components σ_{ij} at the nuclear sites by the fourth-rank gradient-elastic tensor C_{ijkl} , where ϕ_{ij} is equal to

$$\phi_{ij} = \sum_{k,l} C_{ijkl} \sigma_{k,l}, \quad (3)$$

zero in the alkali halide single crystals. Cubic symmetry reduces the number of independent gradient-elastic constants from 81 to 2, and these are C_{11} and C_{44} in the Voight notation.

In the cubic axis system of the crystal, the EFG tensor can be written in the form

$$\begin{aligned} \phi_{x^*x^*} &= C_{11} \left[\sigma_{x^*x^*} - \frac{1}{2} (\sigma_{y^*y^*} + \sigma_{z^*z^*}) \right], \\ \phi_{x^*y^*} &= C_{44} \sigma_{x^*y^*}, \end{aligned} \quad (4)$$

where the subscripts are cyclically permutable. A rotation about the $x^* = x'$ axis to the (x', y', z') coordinates fixed in the laboratory gives

$$\phi_{z'^z'} = -\frac{1}{2} [\phi_{xx} + (\phi_{xx} + 2\phi_{yy}) \cos 2\theta_x], \quad (5)$$

where z' is parallel to the magnetic field H_0 . An additional rotation of the crystal by 45° about x^* transforms (x^*, y^*, z^*) to (x, y, z) ,

$$\phi_{z'^z'} = -\frac{1}{2} \left[\frac{1}{4} C_{11} (1 + 3\gamma) + \frac{1}{2} C_{44} (1 - \gamma) \right] \sigma, \quad (6)$$

where $\gamma = \cos 2\theta_x$ and σ is the nonzero stress component parallel to the $[110]$ rotation axis x . Equation (6) simplifies to

$$\phi_{z'^z'} = -\frac{1}{3} C_{44} \sigma, \quad (7)$$

where z' is parallel to a $[111]$ direction and the uniaxially applied stress component σ is parallel to a $[110]$ axis. In order to determine C_{44} from the NMR data this value for the EFG component is related, in the manner outlined in Ref. 3, to the satellite splitting and second moment defined in Eqs. (1) and (2), respectively. The constant C_{44} is determined (as outlined in Ref. 3) to be 16×10^4 statvolt/dyn. An estimated uncertainty for this value is $\pm 25\%$. A value of 28×10^4 statvolt/dyn was measured for C_{44} in NaI by Astrue and Hooper.⁴

An attempt was made to determine the gradient elastic constant C_{11} by compressing along a $[100]$ axis with H_0 parallel to a $[100]$ axis, but no detectable changes in the NMR line were observed.

VI. EFFECTS OF ORIENTED DISLOCATIONS ON THE ANGULAR POSITION OF THE INTENSITY ANOMALIES IN THE NMR OF ^{127}I IN CsI

A calculation¹⁰ of the quadrupole NMR linewidth for the ^{127}I resonance in CsI is performed as a function of the gradient elastic constants, C_{11} and C_{44} , and the angle of crystal rotation θ . It is assumed that the intensity maxima exist at angles θ , where the quadrupole splitting vanishes or is very

small. Oriented screw- and edge-type dislocations are assumed to cause the orientation-dependent elastic field gradients, and selected dislocation orientations are compared to determine which dislocation orientations are consistent with the $[111]$ and $[100]$ intensity anomalies observed in CsI.

The quadrupole splitting in Eq. (1) is in terms of the EFG component $\phi_{z'^z'}$, where z' is parallel to H_0 . The component $\phi_{z'^z'}$ can be expressed mathematically in terms of a second set of EFG tensor components which are written with respect to coordinate axes imbedded in the crystal [Eq. (2)].

A dislocation coordinate system consisting of three rectangular coordinate axes is imbedded in the crystal. Two of the axes lie in the slip plane and they are parallel to the screw and edge dislocation lines. The third axis is normal to the slip plane and defines its direction in space. The slip direction is defined by the Burger's vector \vec{b} which is parallel to the screw dislocation axis.

Two distinct types of dislocation coordinate systems are considered: the (X, Y, Z) system which contains two perpendicular $[110]$ axes and the cubic axis system (x^*, y^*, z^*) . Screw and edge dislocation lines are oriented along all possible $[110]$ and $[100]$ directions. Six distinct $[110]$ and three distinct $[100]$ orientations exist in a cubic crystal. Each possible dislocation system is considered in conjunction with either a $[100]$ or $[110]$ axis of rotation. A total of 18 distinct cases exist for the $[100]$ and $[110]$ rotation patterns where the dislocation system has either a (100) or (110) slip plane. The cases are further classified according to whether the edge and screw dislocation axes are parallel to $[100]$ or $[110]$ directions.¹⁰

The stress tensor $\sigma_{x^*y^*z^*}$, which is in the cubic axis system fixed in the crystal, is related to the EFG tensor $\phi_{x^*y^*z^*}$ by Eq. (4). The tensor σ_{xyx} is transformed to $\sigma_{x^*y^*z^*}$ by rotating about a $[110]$ axes through 45° . The $\phi_{x^*y^*z^*}$ components can then be related to the $\phi_{z'^z'}$ component using Eq. (2), and the quadrupole splitting $\Delta\nu_m$ is related to $\phi_{z'^z'}$ by Eq. (1). One is thus able to calculate values proportional to the quadrupole splitting of the NMR line which are produced by the stress fields of fixed, oriented screw and edge dislocations in the crystal.

The stress components of edge and screw dislocation¹¹ can be expressed in terms of the cylindrical coordinates (r, α, Z) , where Z is the dislocation axis. Since all the components have the same r dependence, they only differ in their dependence upon α . The second moment of the quadrupole splitting is obtained by averaging over the α variation of the stress components in the crystal

$$\Delta\nu_2^2 \propto \frac{1}{2\pi} \int_0^{2\pi} \phi_{z'^z'}^2 \sin^2 \alpha \, d\alpha, \quad (8)$$

where $(\Delta\nu_2^2)^{1/2}$ is proportional to the rms value of $\phi_{g'g'}$ by Eq. (8). The observable intensity peaks in the [110] and [100] rotation patterns correspond to zero or near zero values of $\Delta\nu_2^2$ in Eq. (8).

The average value $\langle \phi_{g'g'}^2 \rangle$ is calculated as a function of the angle of rotation θ about a fixed axis in the crystal and in terms of C_{11} and C_{44} . For most cases the quantity $\langle \phi_{g'g'}^2 \rangle$ is proportional to terms containing C_{11}^2 and C_{44}^2 . When the crystal is rotated about a [100] direction for the assumed dislocation orientations the quadrupole splitting vanishes for 75% of the cases when H_0 is parallel to a [100] direction. No distinction can be made between a (110) or a (100) slip plane if $C_{44} \gg C_{11}$ since the zeros of $\langle \phi_{g'g'}^2 \rangle$ are the same for both orientations.

In NaI, where C_{44}/C_{11} is approximately 9, a large [100] intensity anomaly is experimentally observed for rotations about a [100] axis. If one calculates the angular variations of $\langle \phi_{g'g'}^2 \rangle$ for dislocations when $C_{44} \gg C_{11}$, it is found that 50% more screw dislocation axes which produce a vanishing quadrupole splitting are parallel to [110] rather than [100] directions. Since the intensity variations are so large for a [100] rotation of NaI, the [110] slip direction seems to be the best choice. One would predict the same slip direction in KI where the ratio of C_{44}/C_{11} is approximately¹² 3 and the [100] intensity maximum for a [100] rotation axis is much smaller. When one considers the [110] rotation in NaI where $C_{44} \gg C_{11}$, then the choice of the [110] screw axis or slip direction is consistent with the vanishing of the quadrupole interaction when H_0 is parallel to a [100] direction and in addition is consistent with the fact that the ratio of maximum to minimum intensities is less (1.25) than 3.9 which is observed for a [100] rotation. In NaI no distinction can be made between a (100) and a (110) slip plane on the basis of the observed [100] intensity anomaly for a [110] rotation and the dislocation axes considered in these calculations.

For CsI the constant C_{11} was measured by acoustic methods¹³ yielding a value of 16.8×10^4 dyn^{-1/2}. The experimental value of C_{44} in CsI given by our

work is approximately 16×10^4 dyn^{-1/2}. The ratio of C_{44}/C_{11} for CsI should then be roughly 1. This indicates that both the C_{11}^2 and the C_{44}^2 terms play an important role in determining the zeros of $\langle \phi_{g'g'}^2 \rangle$. The condition $C_{44} \gg C_{11}$ in NaI must be replaced by C_{11} approximately equal to C_{44} in CsI. The quantity $\langle \phi_{g'g'}^2 \rangle$ vanishes identically for only a few cases when the condition ($C_{11} = C_{44}$) is assumed to hold. It appears that if either a C_{11}^2 or C_{44}^2 term vanishes, a relative minimum in $\langle \phi_{g'g'}^2 \rangle$ exists which is small enough to increase the intensity of the NMR line.

The experimental data for the [110] rotation curves in CsI show rather large [111]-type intensity peaks (Fig. 2). The calculation of $\langle \phi_{g'g'}^2 \rangle$ for the various dislocation orientations indicates that the [100] screw axis is a better choice than a [110] screw axis since more cases vanish when H_0 is parallel to a [111] direction for this slip direction. The CsI crystal structure is body-centered cubic as compared to the face-centered cubic structure of NaI and KI. A [100] slip direction is the most probable slip direction in a body-centered ionic single crystal, and experimentally the cesium halides are observed to slip parallel to these directions.¹⁴

The experimental data for the [100] rotation curves in CsI show a relatively small [100] intensity peak (Fig. 1). Since C_{44}/C_{11} is approximately one for CsI, one would expect a much smaller intensity peak than for NaI. A [100] orientation for the screw axis gives 33% fewer cases than for the [110] orientation where the quadrupole splitting vanishes for H_0 parallel to [100] directions. Also a distinction can not be made between a (100) or (110) slip planes for either of the [110] or [100] rotation curves for CsI.

In summary the calculations outlined above do show that the intensity anomaly in both NaI and CsI can be explained by oriented dislocation of the type described. The dislocation distribution could be different in crystals grown by techniques other than those used by the Harshaw Chemical Co.

*Based on work performed by Grant R. Gerhart in partial fulfillment of the requirements for the Degree of Doctor of Philosophy at Wayne State University.

†Present address: U. S. Army Automotive-Tank Command, Warren, Mich. 48090.

¹G. D. Watkins and R. V. Pound, Phys. Rev. **89**, 658 (1953).

²J. F. Hon and P. J. Bray, J. Appl. Phys. **30**, 1425 (1959).

³H. O. Hooper and P. J. Bray, J. Appl. Phys. **37**, 1633 (1966).

⁴R. W. Astrue and H. O. Hooper, Phys. Rev. **164**, 1206 (1967).

⁵G. M. Volkoff, H. E. Petch, and D. W. Smellie, Can. J. Phys. **30**, 270 (1952).

⁶G. D. Watkins, Ph.D. thesis (Harvard University, 1952) (unpublished).

⁷J. H. Van Vleck, Phys. Rev. **74**, 1168 (1948).

⁸R. V. Pound, Phys. Rev. **79**, 685 (1950).

⁹R. G. Shulman, B. J. Wyluda, and P. W. Anderson, Phys. Rev. **107**, 953 (1957).

¹⁰G. R. Gerhart, Ph.D. thesis (Wayne State University, 1972) (unpublished).

¹¹A. H. Cottrell, *Dislocations and Plastic Flow in Crystals* (Oxford U. P., London, 1953).

¹²E. Otsuka, J. Phys. Soc. Jpn. 13, 1135 (1958).

¹³M. Menes and D. I. Bolef, J. Phys. Chem. Solids 19, 79 (1961).

¹⁴D. Hull, *Introduction to Dislocations* (Pergamon, Oxford, 1965).